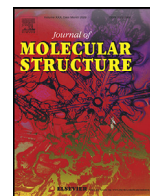




Since January 2020 Elsevier has created a COVID-19 resource centre with free information in English and Mandarin on the novel coronavirus COVID-19. The COVID-19 resource centre is hosted on Elsevier Connect, the company's public news and information website.

Elsevier hereby grants permission to make all its COVID-19-related research that is available on the COVID-19 resource centre - including this research content - immediately available in PubMed Central and other publicly funded repositories, such as the WHO COVID database with rights for unrestricted research re-use and analyses in any form or by any means with acknowledgement of the original source. These permissions are granted for free by Elsevier for as long as the COVID-19 resource centre remains active.



Targeting SARS-CoV-2 main protease by teicoplanin: A mechanistic insight by docking, MM/GBSA and molecular dynamics simulation

Faizul Azam*, Eltayeb E M Eid, Abdulkarim Almutairi

Department of Pharmaceutical Chemistry & Pharmacognosy, Unaizah College of Pharmacy, Qassim University, Saudi Arabia



ARTICLE INFO

Article history:

Received 26 September 2020

Revised 5 July 2021

Accepted 14 July 2021

Available online 18 July 2021

Keywords:

Covid-19

SARS-CoV-2 main protease

Teicoplanin

Docking

Molecular dynamics

ABSTRACT

First emerged in late December 2019, the outbreak of novel severe acute respiratory syndrome corona virus-2 (SARS-CoV-2) pandemic has instigated public-health emergency around the globe. Till date there is no specific therapeutic agent for this disease and hence, the world is craving to identify potential antiviral agents against SARS-CoV-2. The main protease (M^{Pro}) is considered as an attractive drug target for rational drug design against SARS-CoV-2 as it is known to play a crucial role in the viral replication and transcription. Teicoplanin is a glycopeptide class of antibiotic which is regularly used for treating Gram-positive bacterial infections, has shown potential therapeutic efficacy against SARS-CoV-2 *in vitro*. Therefore, in this study, a mechanistic insight of intermolecular interactions between teicoplanin and SARS-CoV-2 M^{Pro} has been scrutinized by molecular docking. Both monomeric and dimeric forms of M^{Pro} was used in docking involving blind as well as defined binding site based on the known inhibitor. Binding energies of teicoplanin- M^{Pro} complexes were estimated by Molecular Mechanics/Generalized Born Surface Area (MM/GBSA) computations from docking and simulated trajectories. The dynamic and thermodynamics constraints of docked drug in complex with target proteins under specific physiological conditions was ascertained by all-atom molecular dynamics simulation of 100 ns trajectory. Root mean square deviation and fluctuation of carbon α chain justified the stability of the bound complex in biological environments. The outcomes of current study are supposed to be fruitful in rational design of antiviral drugs against SARS-CoV-2.

© 2021 Elsevier B.V. All rights reserved.

1. Introduction

The novel coronavirus disease 2019 (COVID-19), caused by severe acute respiratory syndrome coronavirus 2 (SARS-CoV-2), is the third outbreak of human corona viruses which has rapidly engulfed the globe resulting in pandemic situation and widespread public concern [1,2]. Like previously reported severe acute respiratory syndrome coronavirus (SARS-CoV) and Middle East respiratory syndrome coronavirus (MERS-CoV), SARS-CoV-2 is one amongst the β -coronavirus family [3]. COVID-19 is highly contagious and easily transmitted through human-to-human contact with clinical manifestation of fever and pulmonary symptoms. Severely ill patients may suffer from severe acute respiratory syndrome, pneumonia, renal failure, and even death [4]. The disease may exacerbate in case of underlying comorbidities like diabetes, hypertension and other cardiovascular complications which often correlate with detrimental outcomes and poor survival [5]. Till date, there is no specific therapeutic regimen for the treatment of this dev-

astating SARS-CoV-2 infection. Although available medications can only alleviate few symptoms like difficulty in breathing, the world is craving to identify potential antiviral agents or vaccines against SARS-CoV-2 [6].

However, continuing researches on SARS-CoV-2 have certainly provided an understanding of structural information of the key proteins involved in viral life cycle which has accelerated the structure-based drug design approaches aimed at suitable therapeutic development for COVID-19 [7]. Particularly, main protease (M^{Pro}), also called as 3C-like protease or 3CL Pro , is an important proteolytic enzyme belonging to cysteine protease family and one of the structurally well-characterized proteins of SARS-CoV-2 [8,9]. Hampering the functional role of M^{Pro} by small molecule or other peptidomimetic inhibitors has attracted much attention because the enzyme is specifically involved in cleaving polyproteins leading to release of a set of functional non-structural proteins, such as nsp4–nsp16 [9,10]. In addition, targeting M^{Pro} by selected inhibitors seems to be non-toxic in COVID-19 infected patients because no human proteases have been identified having similarity with SARS-CoV-2 specified proteolytic cleavage [7].

Currently, several antivirals, antimalarials, anti-parasitic, and antibacterial agents are in clinical investigations for the treatment

* Corresponding author.

E-mail addresses: f.azam@qu.edu.sa, faizulazam@gmail.com (F. Azam).

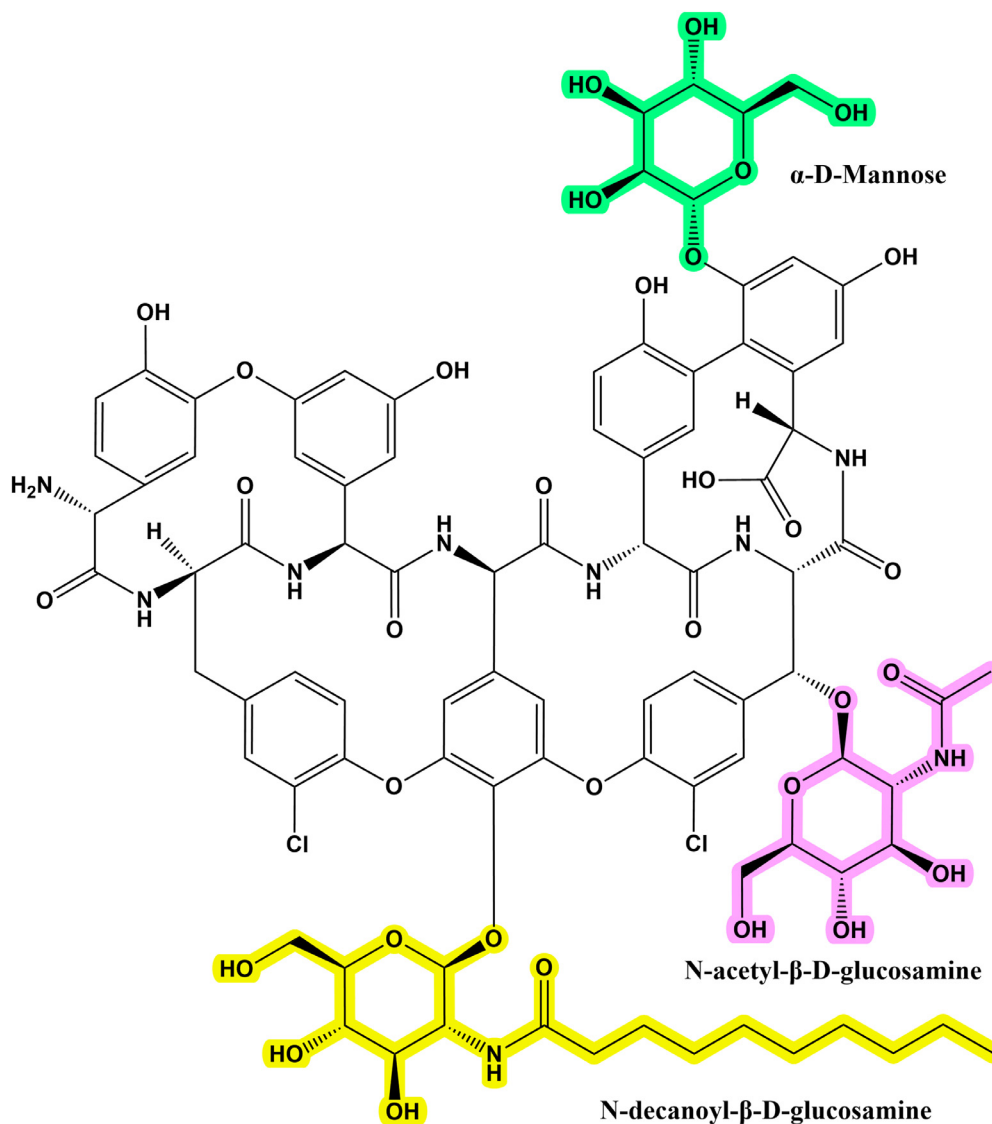


Fig. 1. Chemical structure of the teicoplanin used in present study.

of COVID-19 [11]. In particular, teicoplanin (Fig. 1), a widely available FDA-approved glycopeptide type of antibiotic is known to possess low toxicity profile in humans, is molecule of interest as possible COVID-19 medication. It is routinely used in clinical practice for the treatment of bacterial infections. Interestingly, it has shown antiviral activity against strains of SARS-CoV, MERS-CoV and Ebola viruses [12]. Very recently, same research group has disclosed that teicoplanin can prevent the cellular entry of SARS-CoV-2 at 1.66 μ M concentration [13,14].

Computer-aided drug design techniques are routinely employed in drug design and discovery projects owing to several advantages such as rapid development process and reduced cost [15–17]. In particular, molecular docking coupled with molecular dynamics simulation studies are intended to decipher the mechanism of binding interactions at the molecular levels. Rapid mechanistic insight is vital for understanding structure-activity relationship and lead optimization for the design and discovery of potential molecules [18–20]. In this study, several computational techniques such as molecular docking, Molecular Mechanics-Generalized Born Surface Area (MM-GBSA) and molecular dynamics simulation were exploited to inspect the binding interactions between teicoplanin and SARS-CoV-2 M^{Pro}. The study is envisioned to assist in finding

potential leads and accelerate drug development process for the treatment of novel coronavirus, COVID-19.

2. Materials and methods

2.1. Protein and ligand preparation

Three-dimensional X-ray crystal structure of monomeric form of SARS-CoV-2 M^{Pro} in complex with an inhibitor N-[(5-methylisoxazol-3-yl)carbonyl]alanyl-L-valyl-N-1-((1R,2Z)-4-(benzyloxy)-4-oxo-1-[(3R)-2-oxopyrrolidin-3-yl]methyl)but-2-enyl)-L-leucinamide (N3; PDB ID: 6LU7) and dimeric M^{Pro} (PDB ID: 6WTM) were retrieved from Protein Data Bank [9,21]. Initial processing of the protein structures was performed in Biovia Discovery Studio Visualizer 2020 and PyMOL 1.7.4 for removing the solvent and the co-crystallized molecules. Two-dimensional structure of the teicoplanin was obtained from PubChem database in sdf format (Pubchem ID: 133065662; CAS number: 61036-62-2) and converted to its three-dimensional coordinate by using Open Babel program [22]. Jaguar v10.9 of Schrodinger Suites 2020-3 [23] was used for geometry optimization. The density functional theory (DFT) computation was performed by the hybrid density

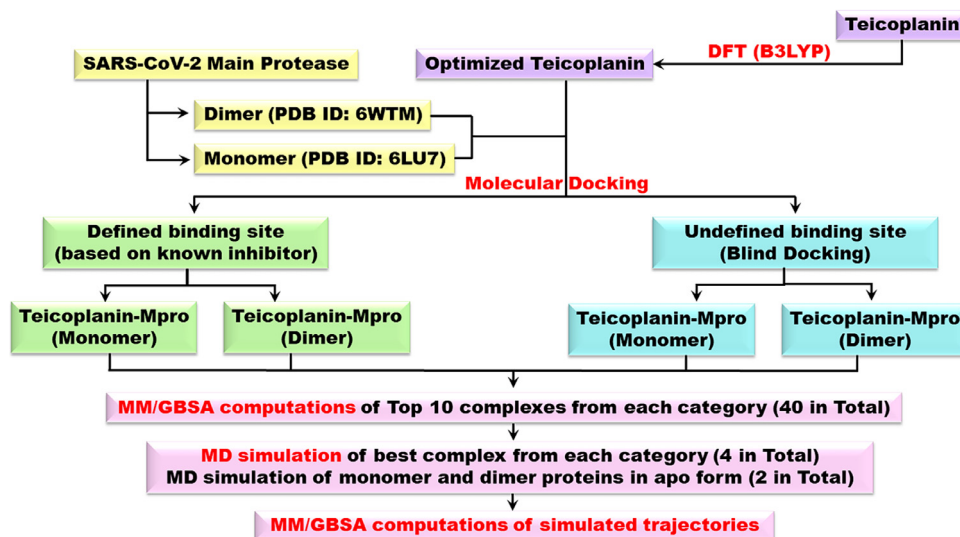


Fig. 2. An outline of the adopted methodology in this study.

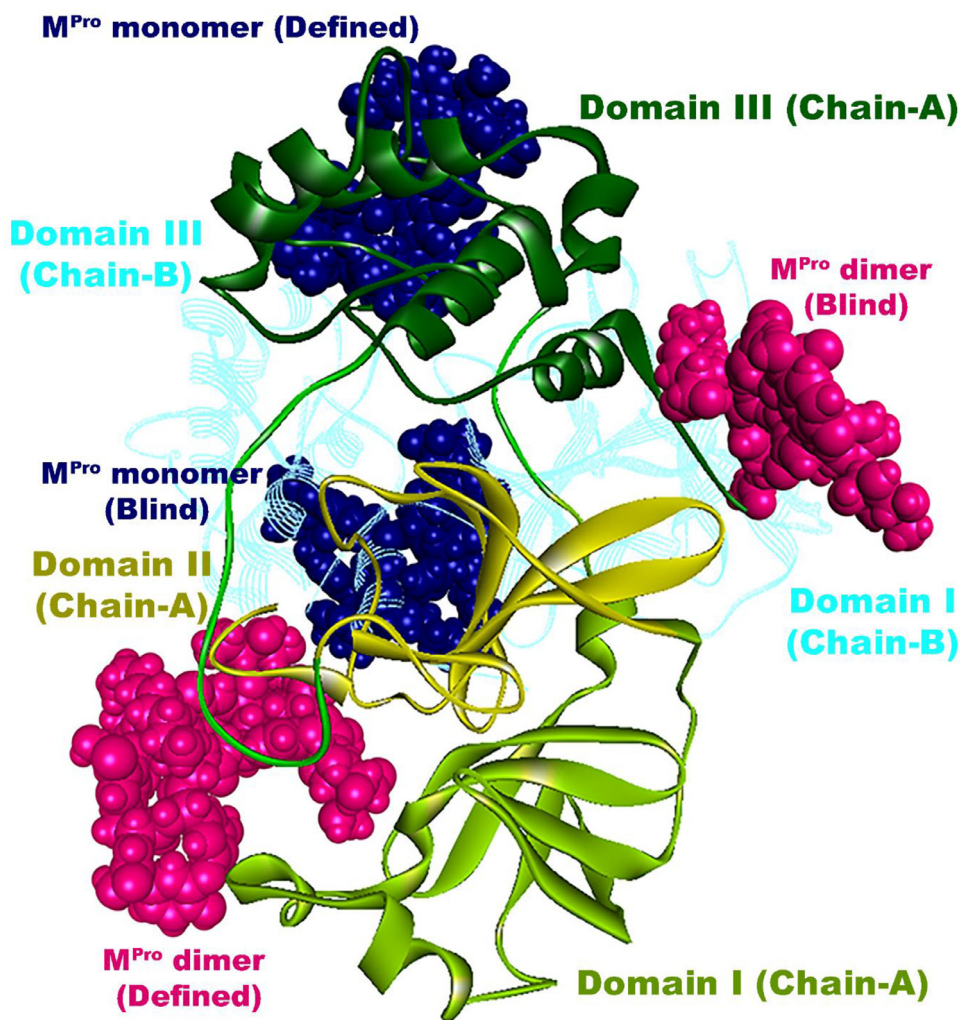


Fig. 3. Best docked poses of the teicoplanin (shown as CPK rendering) in both monomeric and dimeric forms of the M^{Pro}. Teicoplanin docked in monomeric form is represented in dark blue color while dark pink color is used to demonstrate docked teicoplanin in the dimeric protein. Chain A is presented as solid ribbon while chain B has been rendered as line ribbon in cyan color (For interpretation of the references to color in this figure legend, the reader is referred to the web version of this article.).

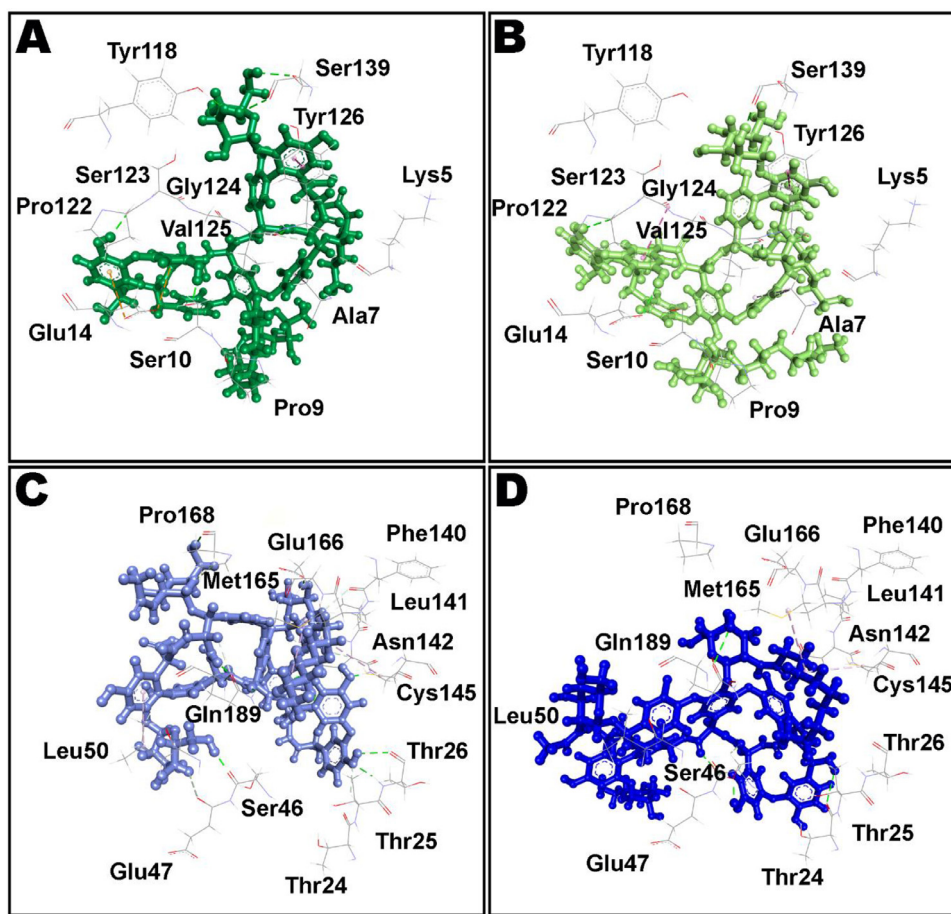


Fig. 4. Teicoplanin in complex with monomeric M^{Pro}. A and B shows blind docking results of first and last frame, respectively. C and D depicts defined docking results of first and last frame, respectively. All frames were extracted from 100 ns MD simulated trajectories.

functional method B3LYP with the 6-311G basis set [24]. The optimized structure of teicoplanin has been presented as Fig. S1 in Supplementary Information. All non-polar hydrogens were merged, rotatable bonds and torsion tree were defined and prepare_ligand4.py module was used to generate pdbqt file with Gasteiger charges added in MGL Tools 1.5.6. The pdbqt file served as input file for AutoDock 4.2. The methodology adopted in this study has been outlined in Fig. 2.

2.2. Molecular docking simulation

AutoGrid 4.2 was employed to calculate numerous grids around both monomeric and dimeric forms of M^{Pro} for both blind and defined dockings having a grid spacing of 0.375 Å. All the parameters of grid points and grid center have been presented as Table S1 in supplementary information. A distance-dependent function for dielectric constant was applied for the computation of energetic maps. Applying the active site information pertaining to the native co-crystallized ligand, N3, a grid box center for defined dockings was established in both monomeric and dimeric forms of M^{Pro}. However, in both proteins, entire macromolecule was considered as the searching site for blind dockings. AutoDock 4.2 was used for docking simulations involving 100 independent runs by Lamarckian genetic algorithm methodology, adjusting default settings for all other parameters [25]. At the end of each docking, ten best poses were individually analyzed for intermolecular interactions using Biovia Discovery Studio Visualizer 2020, and PyMol 1.7.4 programs [20,26] and further subjected to MM/GBSA computations in the next step.

2.3. Prime MM/GBSA calculations

MM/GBSA technique was exploited as a post-docking validation protocol. The binding energy computed by Prime MM/GBSA of Schrödinger Suite 2020-3 [27,28] demonstrates an adequate estimation of binding affinity. The MM/GBSA protocol implemented in Prime combines OPLS molecular mechanics energies, a VSGB solvation model for polar solvation (G_{SGB}), and a nonpolar solvation expression (G_{NP}) involving nonpolar solvent-accessible surface area (SASA) and van der Waals interactions [29]. For each docked teicoplanin-M^{Pro} complex, Prime MM/GBSA estimated the binding free energy (ΔG_{bind}) of teicoplanin according to the equation [30].

$$\Delta G_{bind} = \Delta E_{MM} + \Delta G_{solv} + \Delta G_{SA}$$

Where, ΔE_{MM} is the difference in energy between the complex structure and the sum of the energies of the protein with and without teicoplanin, ΔG_{solv} is the difference in the GBSA solvation energy of the teicoplanin-protein complex and the sum of the solvation energies for the teicoplanin-bound and unbound protein, and ΔG_{SA} is the difference in the energy of surface area for the teicoplanin-M^{Pro} complex and the sum of the surface area energies for the ligand and un-complexed protein.

2.4. Molecular dynamics simulation

The best ranked conformation of teicoplanin furnished by each category of docking experiments in complex with SARS-CoV-2 M^{Pro} was further examined for assessing their thermodynamic behavior and stability by using MD simulation studies employing

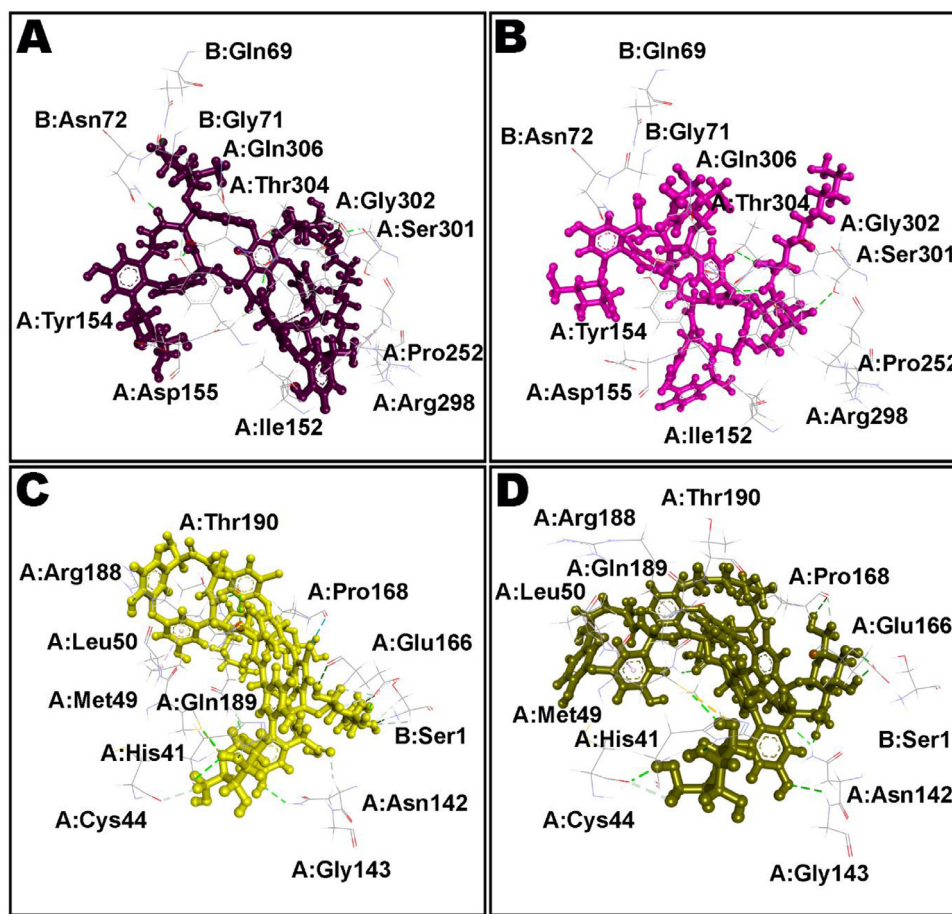


Fig. 5. Teicoplanin in complex with dimeric M^{Pro}. A and B represents blind docking results of first and last frame, respectively. C and D depicts defined docking findings of first and last frame, respectively. All frames were extracted from 100 ns MD simulated trajectories.

Desmond 6.1 program [31,32]. In total, six individual systems were simulated which also includes both monomeric and dimeric forms of apo M^{Pro}. System setup protocol was used for placing the ligand-protein complex or apo protein into an orthorhombic box having 10 Å buffer region between protein atoms and box sides and filled with appropriate number of water molecules (see Table S4 in Supplementary Information). Simple point charge (SPC) model and OPLS3e force field was adopted for the MD computations [33]. Partial charges assigned on each atom of teicoplanin molecule by OPLS3e force field is listed in Table S3 of Supplementary Information. The system was neutralized using appropriate numbers of counter ions (Na⁺ and Cl⁻) with fixed salt concentration of 0.15 M that represents the physiological concentration of monovalent ions. Isothermal-isobaric (NPT) ensemble was employed with temperature and pressure adjusted to 300 K and 1.01325 bar, respectively. A simulation time of 100 ns was adjusted whereas trajectories were saved at every 100 ps. A cut-off radius of 9.0 Å was used for short-range van der Waals and Coulomb interactions. Nose-Hoover thermostat [34] and Martyna-Tobias-Klein [35] methods were employed for maintaining the system temperature and pressure, respectively. Reference system propagator algorithm (RESPA) integrator was used to integrate the equations of motion, with an inner time step of 2.0 fs for bonded as well as non-bonded interactions within the short-range cut-off [36]. Particle Mesh Ewald method was used for accurate and efficient evaluation of electrostatic interactions [37]. The system was minimized and equilibrated with the default protocols of the Desmond. Simulation event analysis, simulation

quality analysis and simulation interaction diagram protocols of the Desmond package was exercised to analyze the trajectory files.

2.5. Post-simulation MM/GBSA analysis

Post-simulation MM/GBSA analysis was performed by using the thermal_MMGBSA.py script of the Prime/Desmond module of the Schrodinger suite 2020-3 [27,28]. From each MD trajectory, every 10th frame was extracted from the last 50 ns of simulated trajectories, averaging over 50 frames, for binding free energy calculations of teicoplanin. The Prime MM/GBSA method uses rule of additivity wherein total binding free energy (Kcal/mol) represents a summation of individual energy modules like coulombic, covalent, hydrogen bond, van der Waals, self-contact, lipophilic, solvation, and π - π stackings of ligand and protein.[38]

3. Results and discussion

3.1. Validation of docking protocol

Validation of the implemented docking protocol in AutoDock 4.2 was performed by re-docking of native co-crystallized ligand, N3 in the binding pocket of SARS-CoV-2 M^{Pro}. The root-mean square deviation (RMSD) of the best docked conformation of N3 and X-ray crystal structure was within 2 Å in this study, confirming the reliability of the implemented scoring function (data not shown). According to the reported protocols, it is evident that the RMSD should fall within ≤ 2.0 Å for a successful docking [39,40].

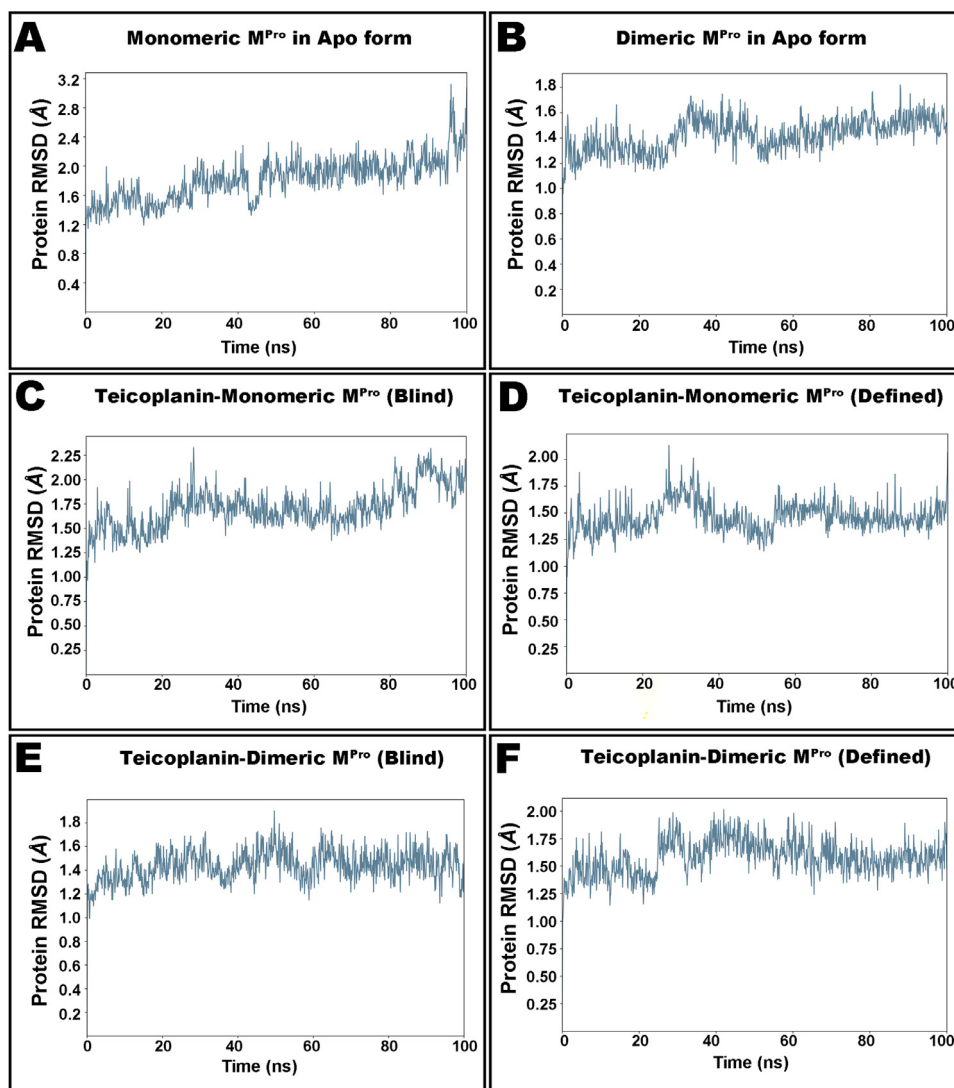


Fig. 6. The root-mean square deviations (RMSD) of α atoms of SARS-CoV-2 main protease in apo form (A,B) and in complex with teicoplanin (C-F) during 100 ns MD simulation.

Therefore, adopted methodology of the molecular docking used in current study, can be relied to predict the molecular interactions of teicoplanin with the SARS-CoV-2 M^{Pro} .

3.2. Molecular docking of teicoplanin with SARS-CoV-2 main protease

Molecular docking is a computer-based process of facilitating the early stages of drug discovery through unveiling the mode of binding interactions of chemical compounds as well as systematic pre-screening on the basis of their shape and energetic compatibility with the target proteins.[17,41] After successful completion of the docking calculations, ten best poses of teicoplanin obtained from each docking run was visualized in Biovia Discovery Studio Visualizer 2020 and PyMol 1.7.4 programs to study ligand–protein interactions. As demonstrated in Table 1, docked teicoplanin had ample opportunity within the SARS-CoV-2 M^{Pro} to interact by means of both hydrophobic as well as hydrophilic interactions.

X-ray crystal structure of SARS-CoV-2 M^{Pro} constitutes three domains comprising 306 amino acid residues [9]. The functional form of M^{Pro} represents a dimeric entity which is simply a repeat unit of the monomeric form comprising chains A and B. Analysis of all

the docking poses implicates that teicoplanin occupies near domain III in both monomeric and dimeric forms if binding site is defined in the docking. However, docking poses of teicoplanin furnished by blind dockings in both proteins utilized mainly domains I and II consisting of residues 8–101 and 102–184, respectively for intermolecular interactions (Fig. 3). Residues of domains I and II form beta-barrels while domain III residues mainly outline alpha-helices. Residues His41 and Cys145 form the catalytic dyad, forming substrate binding region and located at the cleft of domain I and II in which His acts as a proton acceptor while Cys behaves as a nucleophile. Additional structural features include two deeply buried subsites identified as S1 and S2 whereas three shallow subsites are known as S3–S5. The S1 subsite is composed of Phe140, Gly143, Cys145, His163, Glu166 and His172, but S2 contains Thr25, His41 and Cys145 amino acid residues. S3–S5, known as shallow subsites are capable of tolerating different functionalities and are composed of His41, Met49, Met165, Glu166 and Gln189 amino acid residues.[9,42,43]

A combination of numerous H-bond donors/acceptors as well as hydrophobic sites compelled the teicoplanin molecule to interact with the SARS-CoV-2 M^{Pro} . Docking results of monomer presented in Fig. 4 (A for blind and C for defined docking)

clearly depicts the contribution of Leu141, Asn142 and Glu166 for affording H-bond interactions with teicoplanin at the S1 subsite. In addition, Gln189 residue also contributes hydrogen bond interaction, supporting the docked teicoplanin in the shallow subsite (S3–S5) of the binding cavity. However, Leu50,

Cys145 and Met165 participated in hydrophobic contacts in the form of π -alkyl bonds. Furthermore, contribution of Tyr126 was noted in hydrophobic links in the form of π - π stacking interactions while amide- π stacked interactions were also noted with Ser123 and Gly124 residues. In case of dimeric protein,

Table 1

Non-bond interactions of teicoplanin-M^{Pro} complexes from first and last frames of 100ns MD simulation.

Target	H-Bonds Compd	Amino acid	Dist ^d	Hydrophobic/Electrostatic Type	Amino acid	Dist ^d
M ^{Pro} monomer	H	Lys5	2.42	π -Alkyl	Ala7	5.19
Frame 1	H	Ser10	1.71	π -Anion	Glu14	4.25
(Blind)	O	Tyr118	1.69	π -Anion	Glu14	4.48
	HO	Pro122	2.12	π - π Stacked	Tyr126	4.17
	H	Val125	1.73			
	H	Val125	2.83			
	H	Val125	2.68			
	H	Ser139	2.43			
	H	Ser139	2.52			
M ^{Pro} monomer	O	Pro9	1.79	Alkyl	Met6	4.54
Frame 1	H	Glu14	2.49	Alkyl	Met6	4.57
1001	HO	Pro122	2.60	π -Alkyl	Ala7	5.41
(Blind)	H	Val125	1.92	Alkyl	Ala7	5.45
	H	Val125	2.92	Amide- π Stacked	Ser123:Gly124	4.36
	H	Ser139	1.98	π - π Stacked	Tyr126	5.05
	O	Ser139	2.73			
M ^{Pro} monomer	O	Thr25	2.66	π -Alkyl	Leu50	5.35
Frame 1	O	Thr26	2.02	Alkyl	Cys145	5.27
(Defined)	H	Ser46	1.80	Alkyl	Met165	4.36
	O	Leu141	2.37			
	O	Asn142	2.51			
	H	Asn142	1.78			
	H	Asn142	1.88			
	H	Asn142	2.79			
	O	Asn142	2.21			
	O	Asn142	1.95			
	O	Gly143	1.75			
	O	Gly143	2.49			
	H	Glu166	1.92			
	H	Pro168	2.19			
	O	Pro168	2.65			
	H	Pro168	1.87			
	H	Gln189	2.54			
	O	Gln189	1.86			
	H	Gln189	1.64			
M ^{Pro} monomer	H	Thr24	2.47	π -Alkyl	His41	5.44
Frame 1	H	Thr45	3.07	Alkyl	Cys145	4.38
1001	O	Ser46	2.77	Alkyl	Met165	4.79
(Defined)	H	Ser46	1.96			
	O	Ser46	1.71			
	H	Gln189	1.84			
M ^{Pro} dimer	HO	A:Ile152	2.27	Alkyl	A:Pro252	4.31
Frame 1	H	A:Tyr154	1.98	π -Alkyl	A:Arg298	5.21
(Blind)	H	A:Tyr154	2.82	π -Alkyl	A:Val303	4.73
	O	A:Tyr154	2.44	π - π T-shaped	A:Phe305	5.38
	H	A:Asp155	1.76			
	H	A:Asp155	2.56			
	H	A:Ser301	2.03			
	H	A:Gly302	2.50			
	H	A:Gly302	2.97			
	H	A:Gly302	2.72			
	O	A:Val303	3.04			
	H	A:Thr304	1.72			
	H	A:Thr304	1.98			
	O	B:Gln69	1.65			
	O	B:Gly71	2.65			
	O	B:Asn72	1.63			
M ^{Pro} dimer	H	A:Tyr154	2.69	π - π Stacked	A:Tyr154	5.21
Frame 1	H	A:Tyr154	2.79	π -Alkyl	A:Tyr154	4.80
1001	H	A:Ser301	2.61			
(Blind)	H	A:Ser301	1.72			
	H	A:Ser301	2.90			
	H	A:Gly302	2.51			
	H	A:Thr304	2.92			
	O	A:Gln306	2.78			

(continued on next page)

Table 1 (continued)

Target	H-Bonds Compd	Amino acid	Dist ^d	Hydrophobic/Electrostatic Type	Amino acid	Dist ^d
M ^{Pro} dimer Frame 1 (Defined)	H	A:His41	3.05	π -Alkyl	A:Leu50	3.91
	H	A:His41	1.92			
	H	A:Cys44	2.72			
	H	A:Met49	2.39			
	H	A:Asn142	2.40			
	H	A:Asn142	2.65			
	H	A:Glu166	2.83			
	H	A:Glu166	1.85			
	O	A:Glu166	2.41			
	H	A:Glu166	2.70			
	H	A:Glu166	2.89			
	O	A:Arg188	2.11			
	O	A:Gln189	2.10			
	H	A:Gln189	1.95			
	H:O	A:Thr190	2.69			
	H	A:Thr190	2.70			
	H	A:Thr190	1.83			
	O	B:Ser1	3.02			
	O	B:Ser1	2.51			
	O	B:Ser1	2.19			
M ^{Pro} dimer Frame 1001 (Defined)	O	A:His41	1.79	π -Alkyl	A:Leu50	5.20
	H	A:Cys44	2.70			
	H	A:Cys44	2.05			
	H	A:Met49	2.60			
	O	A:Asn142	2.38			
	O	A:Asn142	1.83			
	O	A:Gly143	2.83			
	H	A:Glu166	1.79			
	H	A:Glu166	1.88			
	H	A:Pro168	2.70			
	H	A:Pro168	2.33			
	O	A:Gln189	2.17			
	H	A:Gln189	1.78			

involvement of His41 of catalytic dyad was observed for establishing polar interaction with teicoplanin in defined docking (Fig. 5).

3.3. Prime MM/GBSA calculations

In computer-aided drug discovery projects, several docking programs are routinely employed for interpreting the binding mode and the affinity of a ligand relative to a protein. However, the binding energy predicted by docking algorithms cannot be relied and hence, it is imperative to employ post-docking analyses to avoid false negatives and false positives [44]. Nowadays, MM/GBSA method is frequently used for predicting the accurate binding energy of a protein-ligand complex and the obtained results can be exploited more rationally in the design of drug candidates [45,46]. Therefore, the top ten poses of SARS CoV-2 M^{Pro}-teicoplanin complexes obtained from hundred docking runs in each category were further analysed by MM/GBSA approach for prediction of more accurate binding energy. In addition, Coulomb binding free energy, hydrogen bonding free energy, the lipophilic binding free energy, the generalized Born solvation binding free energy, the van der Waals binding free energy, and ligand strain energy were also computed and presented as Table S2 in Supplementary Information. Post-docking optimization of several teicoplanin poses obtained from AutoDock 4.2 in complex with both monomeric and dimeric M^{Pro} exhibited MM/GBSA binding energy in the range of -59 to -76 kcal/mol (Table 2). However, MM/GBSA binding energy of -97.55 kcal/mol has been recently reported for the teicoplanin conformation afforded by AutoDock Vina 1.1.2 in complex with monomeric M^{Pro} [47]. The binding energies of the single best pose selected from ten MM/GBSA-optimized conformations belonging to each category of teicoplanin-M^{Pro} com-

plexes are displayed in Table 2. The MM/GBSA results of snapshots from the MD trajectories along with standard deviation calculated from the last 50 frames are also demonstrated in Table 2.

3.4. Molecular dynamics simulation studies

Dynamic and thermodynamics parameters of living systems under specific conditions of physiological environments can be estimated by the application of molecular dynamics (MD) simulation, a widely employed computer-aided drug design technique [17,18,48]. Therefore, the best docked pose of teicoplanin in complex with SARS-CoV-2 M^{Pro} was subjected to MD simulation study in order to investigate the stability of the ligand-protein complex as well as main intermolecular interactions during the simulated trajectory. Each docking pose representing monomer-blind, monomer-defined, dimer-blind and dimer-defined was subjected to MD simulation study owing to the minimum binding energy in MM/GBSA analysis (see Table S2 of supplementary information). In addition, apo form of both monomeric and dimeric forms of M^{Pro} were also simulated for comparative analysis. Desmond software was employed for the MD simulation of 100 ns in explicit solvent system. The resulting trajectories of the simulated complexes were inspected for different standard simulation parameters such as backbone RMSDs for alpha-carbon atoms. In addition, the root-mean square fluctuations (RMSFs) of individual amino acid residues, intermolecular interactions involved, solvent accessible surface area (SASA) and radius of gyration (rGyr) were also evaluated. The RMSD plot of simulated complex is presented in Fig. 6. The analysis of RMSD indicates that the simulated system has equilibrated very well because the fluctuations in the C α atoms were consistently below 2.5 Å during the entire simulated path of all

Table 2
MM/GBSA-computed binding energies of teicoplanin-M^{Pro} complexes obtained from docking and snapshots from the molecular dynamics trajectories.

Targets	Binding energy of docked conformation ^a (Kcal/mol)	Binding energy calculated from snapshots of the molecular dynamics trajectories (Kcal/mol) ^b
M ^{Pro} monomer (Blind)	-73	-127 ± 11
M ^{Pro} monomer (Defined)	-68	-95 ± 8
M ^{Pro} dimer (Blind)	-76	-105 ± 15
M ^{Pro} dimer (Defined)	-59	-96 ± 6

^a Each value corresponds to single best pose selected from ten MM/GBSA-optimized conformations in each category of ligand-protein complexes obtained from AutoDock 4.2.

^b Values represent average ± standard deviation calculated from last 50 frames of 100 ns molecular dynamics simulation.

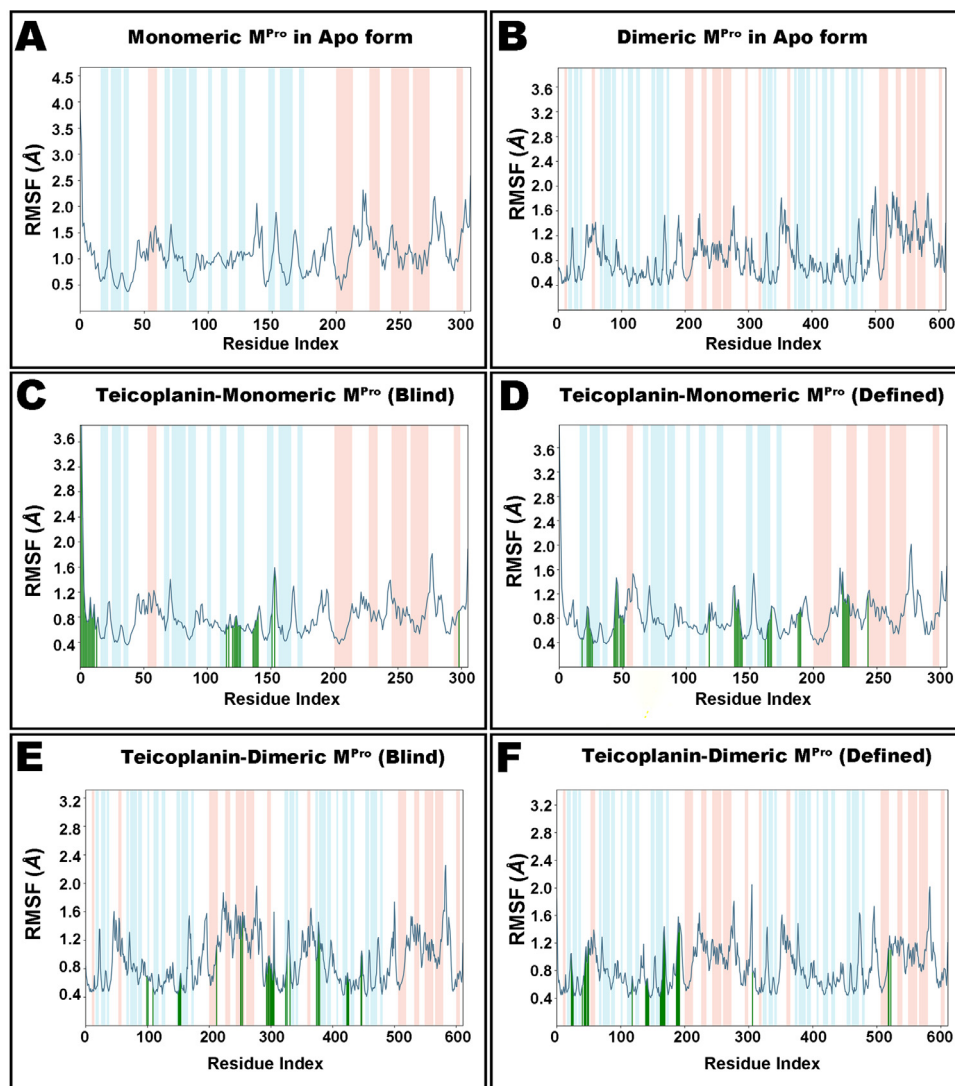


Fig. 7. The root-mean square fluctuation (RMSF) of C α atoms of SARS-CoV-2 main protease in apo form (A,B) and in complex with teicoplanin (C–F) during 100 ns MD simulation. The point of contact of teicoplanin with protein residues is shown by vertical green lines on X-axis. Loop regions are shown by white bar whereas alpha-helices and beta-sheets are represented in the form of blue and pink bars, respectively (For interpretation of the references to color in this figure legend, the reader is referred to the web version of this article.).

complexes. However, slight fluctuation can be expected during initial period which acquires stability throughout rest of simulation route. A system showing fluctuation of 1–3 Å is usually considered stable and deemed to be properly equilibrated in case of globular proteins whereas elevated RMSD values are regarded as an indication of large conformational changes in protein structure over the progression of simulation. Snapshots taken at the inter-

vals of every 20 ns are presented in Fig. S2–S5 of supplementary information.

The local conformational alterations along SARS-CoV-2 M^{Pro} chain were investigated by analyzing the RMSF during simulation time. Loop regions in the RMSF plot has been shown by white bar whereas alpha-helices and beta-sheets are represented in the form of blue and pink bars, respectively. As depicted in

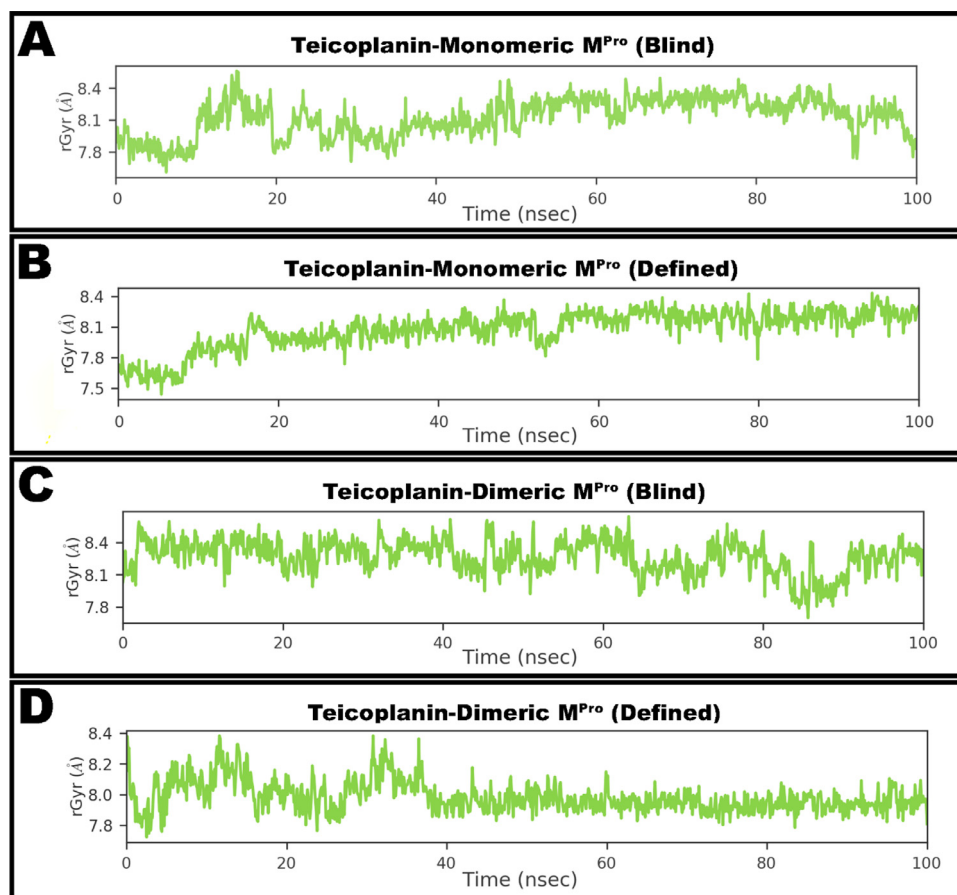


Fig. 8. Radius of gyration (rGyr, shown in Å unit) of numerous complexes of teicoplanin with M^{Pro} during simulated period of 100 ns.

Fig. 7. loop regions usually fluctuate the most during simulation, though alpha-helices and beta-sheets were rigid. The vertical green lines on the X-axis of the plot illustrate the participation of interacting residues between SARS-CoV-2 M^{Pro} chain and teicoplanin. Key residues of H-bond interactions with monomeric M^{Pro} such as Thr24, Thr45, Ser46, Pro122, Val125, Ser139, and Gln189 exhibited maximum RMSFs of 0.96, 1.09, 1.46, 0.79, 0.66, 0.75, and 0.87 Å, respectively. Important residues sharing hydrophobic interactions in this protein such as His41, Ser123, Gly124, Tyr126, Cys145 and Met165 displayed RMSFs of 0.48, 0.79, 0.82, 0.66, 0.49 and 0.69 Å, respectively. All of these figures were estimated around the flexible loop regions of target protein. However, in blind docking complex with dimeric protein, residues such as Ser301, Gly302, Thr304 and Gln306 were among the terminal amino acids and exhibited RMSF of 0.81, 0.87, 0.64 and 1.59 Å, respectively. In addition, Tyr154 participated in both hydrophilic and π - π stacking interactions fluctuated at 0.69 Å. Defined docking complex of teicoplanin with dimeric M^{Pro} participating in hydrogen bonds with His41, Cys44, Met49, Asn142, Gly143, Glu166, Pro168 and Gln189 fluctuated at 0.58, 0.73, 0.91, 0.68, 0.69, 0.68, 1.35 and 1.15 Å, respectively.

Structural compactness of the SARS-CoV-2 M^{Pro} during MD simulation course was established by evaluation of the rGyr. Time-dependency plot of the rGyr for the simulated system comprising docked teicoplanin in complex with SARS-CoV-2 M^{Pro} is shown in **Fig. 8**. Moreover, solvent accessible surface area (SASA) of the complexes under study as a function of simulation time was also studied and presented **Fig. 9**.

Simulation interactions diagrams presented in B and D panels of **Figs. 4** and **5** during entire simulation time signifies a comprehen-

sive intermolecular interaction profile of teicoplanin with SARS-CoV-2 M^{Pro}. The modus of interaction pattern of teicoplanin clearly illustrates that the docking predicted main contacts are nearly preserved throughout the MD simulation time of 100 ns (**Figs. 10** and **11**).

3.4.1. MM/GBSA computations from MD trajectories

Post-simulation MM/GBSA was computed from frame 501–1001 at every 10th frame, totalling 50 conformations of each simulated complex and average binding energies with standard deviation has been tabulated in **Table 2**. MM/GBSA is very popular and rigorous method for post-simulation binding free energy prediction because it considers protein flexibility, entropy, solvation and polarizability, usually unaccounted in several docking protocols and hence, more accurate than most scoring functions implemented in molecular docking. A precise computation of the free energy of binding is one of the most important missions in biomolecular studies because it is responsible for driving all molecular processes, like chemical reaction, molecular recognition, association and protein folding [49]. In both monomeric and dimeric proteins, the estimated binding energies for blind docking were recorded as -127 ± 11 and -105 ± 15 Kcal/mol, respectively. However, in defined docking, the values were observed as -95 ± 8 and -96 ± 6 Kcal/mol for monomer and dimer, respectively.

A number of studies involving drug repurposing strategies employed *in silico* techniques to reveal a large number of small molecules as prospective inhibitors of M^{Pro} (**Table 3**). Gahlawat et al [50], implemented a high-throughput virtual screening of 2454 FDA-approved drugs and identified lithospermic acid B

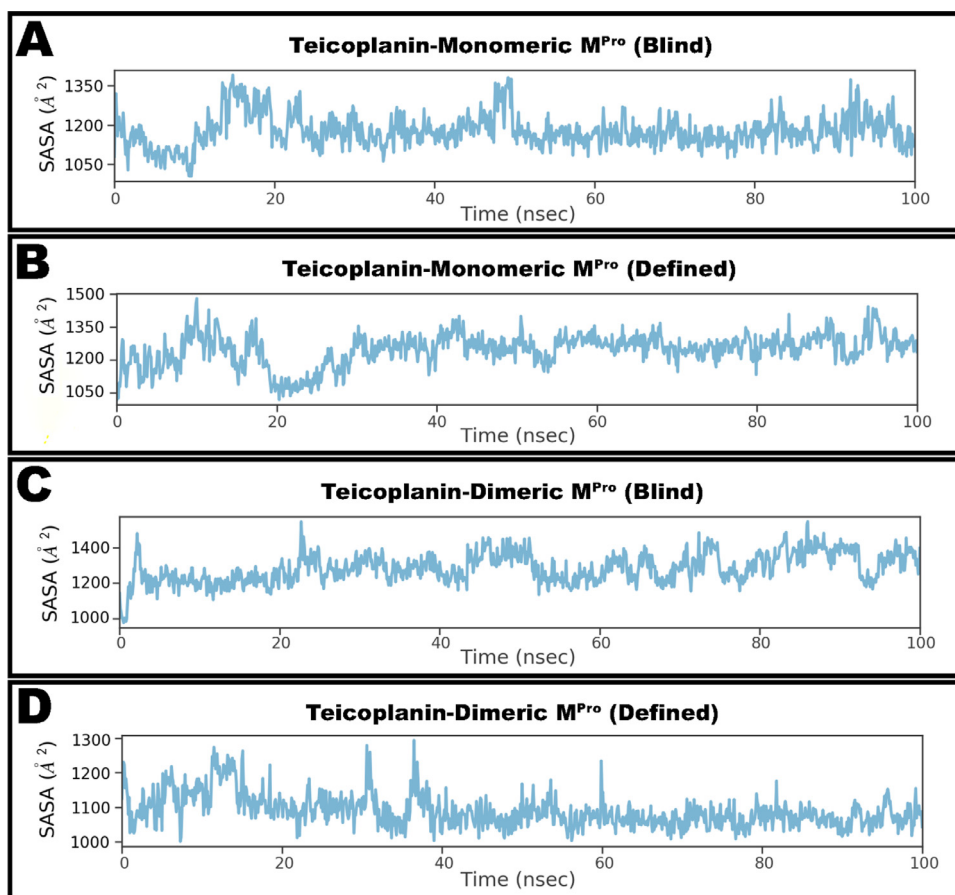


Fig. 9. Solvent accessible surface area (SASA, depicted in Å²) of numerous complexes of teicoplanin with M^{Pro} during simulated period of 100 ns.

Table 3

MM/GBSA binding energies of reported molecules targeting SARS-CoV-2 M^{Pro}.

S.No.	Compound ^a	MM/GBSA binding energies (Kcal/mol)	References
1	Lithospermic acid B	-118.7	[50]
2	Ritonavir	-107.6	[51]
3	AT1001	-106.3	[54]
4	GHRP-2	-106.0	[55]
5	Rutin	-99.8	[52]
6	N3	-80.0	[56]
7	ChemDiv_D658-0159	-77.5	[57]
8	Amikacin	-73.8	[53]
9	γ-glutamyl-S-allylcysteine	-72.5	[58]
10	ZINC000003947429	-70.4	[59]
11	PubChem-129-716-607	-69.0	[60]
12	11b	-65.6	[61]

^a Compound name has been kept same as reported in respective literature.

as one of the suitable candidate for M^{Pro} inhibition exhibiting a binding energy of -118.7 kcal/mol which was calculated from last 20 ns of MD trajectories. In addition, few well-known molecules such as ritonavir, rutin and amikacin were also repurposed against SARS-CoV-2 M^{Pro}, displaying MM/GBSA binding energies of -107.6 kcal/mol [51], -99.8 kcal/mol [52], and -73.8 kcal/mol [53], respectively, which were computed from several snapshots of MD trajectories. Therefore, the binding energies of teicoplanin-M^{Pro} complexes reported hereby using robust computational techniques, are in the agreement with literature values computed on diverse repurposed molecules targeting SARS-CoV-2 M^{Pro} and hence, if tested experimentally, can yield promising results.

4. Conclusions

By using computer-aided drug design techniques, current study explains the intermolecular interaction of antibacterial drug, teicoplanin with SARS-CoV-2 M^{Pro}. Molecular docking studies employing AutoDock 4.2 highlights the importance of hydrophilic and hydrophobic interactions in supporting the teicoplanin molecule inside the SARS-CoV-2 M^{Pro}. MM/GBSA analysis and molecular dynamics simulation results not only reinforce the credibility of the docking results, but also authenticate the stability of the simulated system, supporting the potential *in vitro* inhibitory activity of teicoplanin against SARS-CoV-2. This study is expected to assist lead optimization and design of COVID-19 drugs.

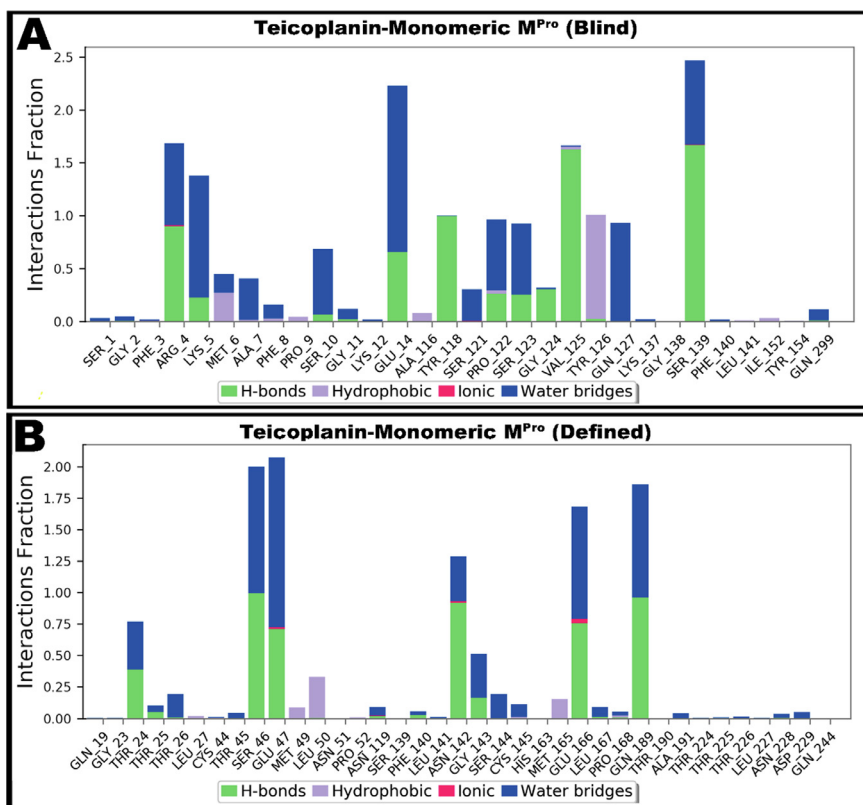


Fig. 10. Monomeric M^{Pro} interactions with teicoplanin, monitored throughout the simulation trajectories. These interactions are clustered by type and summarized in bar diagram including H-bonds, hydrophobic, ionic and water bridges.

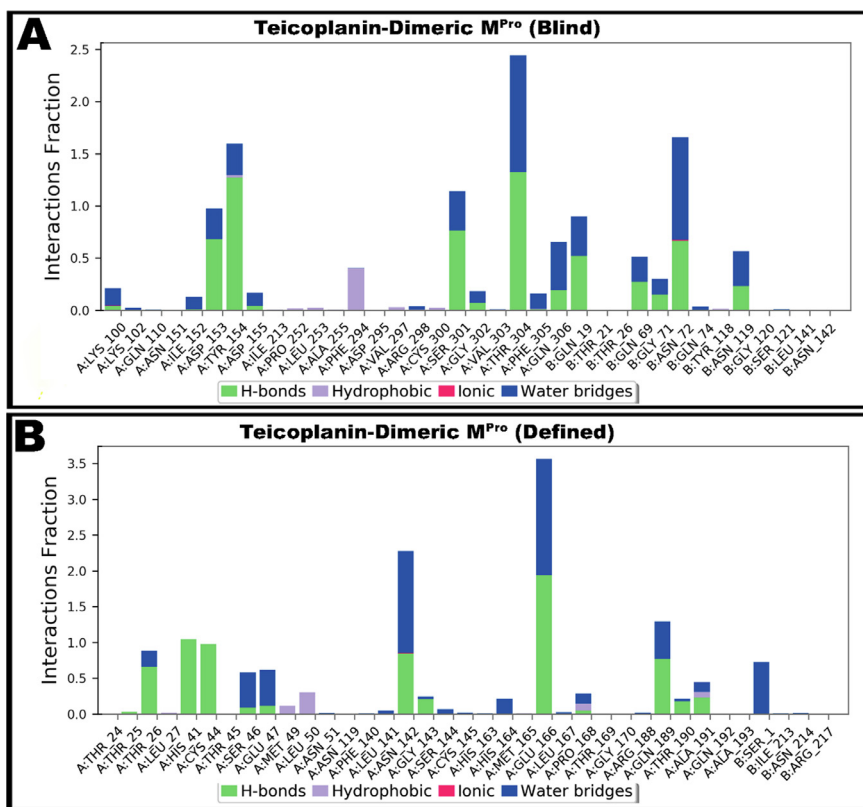


Fig. 11. Dimeric M^{Pro} interactions with teicoplanin, monitored throughout the simulation trajectories. These interactions are clustered by type and summarized in bar diagram including H-bonds, hydrophobic, ionic and water bridges.

Contributions

Faizul Azam: Conceptualization, Methodology, Formal analysis, Software, Validation, Writing, Editing and Funding acquisition. **Eltayeb Eid:** Project administration, Funding acquisition and Revision. **Abdulkarim Almutairi:** Visualization, Data curation and Writing-first draft.

Disclosure statement

No potential conflict of interest was reported by the authors.

Declaration of Competing Interest

The authors declare that they have no known competing financial interests or personal relationships that could have appeared to influence the work reported in this paper.

CRedit authorship contribution statement

Faizul Azam: Conceptualization, Methodology, Formal analysis, Software, Validation, Writing – review & editing, Funding acquisition. **Eltayeb E M Eid:** Project administration, Funding acquisition. **Abdulkarim Almutairi:** Visualization, Data curation, Writing – original draft.

Acknowledgements

The authors gratefully acknowledge the financial support for this study from the Qassim University, Saudi Arabia, represented by the deanship of scientific research (grant no. phuc-2020-1-1-L-10063) during the academic year 1441 AH/2020 AD. Authors are thankful to Schrodinger India for providing the access to Schrodinger Suite 2020-3. Dr Prajwal Nandekar and Dr Sudharshan Pandiyan are kindly acknowledged for their help and support.

Supplementary materials

Supplementary material associated with this article can be found, in the online version, at doi:10.1016/j.molstruc.2021.131124.

References

- [1] D.S. Hui, E.I. Azhar, T.A. Madani, F. Ntoumi, R. Kock, O. Dar, G. Ippolito, T.D. Mchugh, Z.A. Memish, C. Drosten, A. Zumla, E. Petersen, The continuing 2019-nCoV epidemic threat of novel coronaviruses to global health – the latest 2019 novel coronavirus outbreak in Wuhan, China, *Int. J. Infect. Dis.* 91 (2020) 264–266, doi:10.1016/j.ijid.2020.01.009.
- [2] N. Chen, M. Zhou, X. Dong, J. Qu, F. Gong, Y. Han, Y. Qiu, J. Wang, Y. Liu, Y. Wei, J. Xia, T. Yu, X. Zhang, L. Zhang, Epidemiological and clinical characteristics of 99 cases of 2019 novel coronavirus pneumonia in Wuhan, China: a descriptive study, *Lancet* 395 (2020) 507–513, doi:10.1016/S0140-6736(20)30211-7.
- [3] J. Zheng, SARS-CoV-2: an emerging coronavirus that causes a global threat, *Int. J. Biol. Sci.* 16 (2020) 1678–1685, doi:10.7150/ijbs.45053.
- [4] N.C. Peeri, N. Shrestha, M.S. Rahman, R. Zaki, Z. Tan, S. Bibi, M. Baghbanzadeh, N. Aghamohammadi, W. Zhang, U. Haque, The SARS, MERS and novel coronavirus (COVID-19) epidemics, the newest and biggest global health threats: what lessons have we learned? *Int. J. Epidemiol.* 49 (2020) 717–726, doi:10.1093/ije/dyaa033.
- [5] P.-H. Tsai, W.-Y. Lai, Y.-Y. Lin, Y.-H. Luo, Y.-T. Lin, H.-K. Chen, Y.-M. Chen, Y.-C. Lai, L.-C. Kuo, S.-D. Chen, K.-J. Chang, C.-H. Liu, S.-C. Chang, F.-D. Wang, Y.-P. Yang, Clinical manifestation and disease progression in COVID-19 infection, *J. Chin. Med. Assoc.* 84 (2021) https://journals.lww.com/jcma/Fulltext/2021/01000/Clinical_manifestation_and_disease_progression.in.2.aspx.
- [6] D. Raoult, P.-R. Hsueh, S. Stefani, J.-M. Rolain, COVID-19 therapeutic and prevention, *Int. J. Antimicrob. Agents* 55 (2020) 105937, doi:10.1016/j.ijantimicag.2020.105937.
- [7] G.U. Jeong, H. Song, G.Y. Yoon, D. Kim, Y.-C. Kwon, Therapeutic strategies against COVID-19 and structural characterization of SARS-CoV-2: a review, *Front. Microbiol.* 11 (2020) 1723, doi:10.3389/fmicb.2020.01723.
- [8] L. Zhang, D. Lin, X. Sun, U. Curth, C. Drosten, L. Sauerhering, S. Becker, K. Rox, R. Hilgenfeld, Crystal structure of SARS-CoV-2 main protease provides a basis for design of improved α -ketoamide inhibitors, *Science* 368 (2020) 409–412 (80-), doi:10.1126/science.abb3405.
- [9] Z. Jin, X. Du, Y. Xu, Y. Deng, M. Liu, Y. Zhao, B. Zhang, X. Li, L. Zhang, C. Peng, Y. Duan, J. Yu, L. Wang, K. Yang, F. Liu, R. Jiang, X. Yang, T. You, X. Liu, X. Yang, F. Bai, H. Liu, X. Liu, L.W. Guddat, W. Xu, G. Xiao, C. Qin, Z. Shi, H. Jiang, Z. Rao, H. Yang, Structure of Mpro from SARS-CoV-2 and discovery of its inhibitors, *Nature* 582 (2020) 289–293, doi:10.1038/s41586-020-2223-y.
- [10] M.M. Ghahremanpour, J. Tirado-Rives, M. Deshmukh, J.A. Ippolito, C.-H. Zhang, I. Cabeza de Vaca, M.-E. Liosi, K.S. Anderson, W.L. Jorgensen, Identification of 14 Known drugs as inhibitors of the main protease of SARS-CoV-2, *ACS Med. Chem. Lett.* 11 (2020) 2526–2533, doi:10.1021/acsmchemlett.0c00521.
- [11] C. Harrison, Coronavirus puts drug repurposing on the fast track, *Nat. Biotechnol.* 38 (2020) 379–381, doi:10.1038/d41587-020-00003-1.
- [12] N. Zhou, T. Pan, J. Zhang, Q. Li, X. Zhang, C. Bai, F. Huang, T. Peng, J. Zhang, C. Liu, L. Tao, H. Zhang, Glycopeptide antibiotics potently inhibit cathepsin L in the late endosome/lysosome and block the entry of Ebola virus, middle east respiratory syndrome coronavirus (MERS-CoV), and severe acute respiratory syndrome coronavirus (SARS-CoV), *J. Biol. Chem.* 291 (2016) 9218–9232, doi:10.1074/jbc.M116.716100.
- [13] J. Zhang, X. Ma, F. Yu, J. Liu, F. Zou, T. Pan, H. Zhang, Teicoplanin potentially blocks the cell entry of 2019-nCoV, *BioRxiv* (2020), doi:10.1101/2020.02.05.935387.
- [14] S.A. Baron, C. Devaux, P. Colson, D. Raoult, J.-M. Rolain, Teicoplanin: an alternative drug for the treatment of COVID-19? *Int. J. Antimicrob. Agents.* 55 (2020) 105944, doi:10.1016/j.ijantimicag.2020.105944.
- [15] M.A. Ahmed, F. Azam, A.M. Rghigh, A. Gbaj, A.E. Zetrini, Structure-based design, synthesis, molecular docking, and biological activities of 2-(3-benzoylphenyl) propanoic acid derivatives as dual mechanism drugs, *J. Pharm. Bioallied Sci.* 4 (2012), doi:10.4103/0975-7406.92728.
- [16] F. Azam, N. Mohamed, F. Alhussen, Molecular interaction studies of green tea catechins as multitarget drug candidates for the treatment of Parkinson's disease: computational and structural insights, *Network* 26 (2015) 97–115, doi:10.3109/0954898X.2016.1146416.
- [17] F. Azam, N.H. Alabdullah, H.M. Ehedmat, A.R. Abulifa, I. Taban, S. Upadhyayula, NSAIDs as potential treatment option for preventing amyloid β toxicity in Alzheimer's disease: an investigation by docking, molecular dynamics, and DFT studies, *J. Biomol. Struct. Dyn.* 36 (2018) 2099–2117.
- [18] F. Azam, H.S. Abodabos, I.M. Taban, A.R. Rfieda, D. Mahmood, M.J. Anwar, S. Khan, N. Sizochenko, G. Poli, T. Tuccinardi, Rutin as promising drug for the treatment of Parkinson's disease: an assessment of MAO-B inhibitory potential by docking, molecular dynamics and DFT studies, *Mol. Simul.* 45 (2019) 1563–1571.
- [19] M.A.M. Shushni, F. Azam, U. Lindequist, Oxasetin from lophiostoma sp. of the Baltic sea: identification, in silico binding mode prediction and antibacterial evaluation against fish pathogenic bacteria, *Nat. Prod. Commun.* 8 (2013).
- [20] F. Azam, M. Vijaya Vara Prasad, N. Thangavel, A. Kumar Shrivastava, G. Mohan, Structure-based design, synthesis and molecular modeling studies of thiazolyl urea derivatives as novel anti-parkinsonian agents, *Med. Chem.* 8 (2012) 1057–1068 (Los Angeles), doi:10.2174/1573406411208061057.
- [21] W. Vuong, M.B. Khan, C. Fischer, E. Arutyunova, T. Lamer, J. Shields, H.A. Safran, R.T. McKay, M.J. van Belkum, M.A. Joyce, H.S. Young, D.L. Tyrrell, J.C. Vederas, M.J. Lemieux, Feline coronavirus drug inhibits the main protease of SARS-CoV-2 and blocks virus replication, *Nat. Commun.* 11 (2020) 4282, doi:10.1038/s41467-020-18096-2.
- [22] N.M. O'Boyle, M. Banck, C.A. James, C. Morley, T. Vandermeersch, G.R. Hutchison, Open babel: an open chemical toolbox, *J. Cheminform.* 3 (2011) 33, doi:10.1186/1758-2946-3-33.
- [23] Schrödinger Release 2020-3, Schrödinger, LLC, New York, NY, 2020.
- [24] A.D. Bochevarov, E. Harder, T.F. Hughes, J.R. Greenwood, D.A. Braden, D.M. Philipp, D. Rinaldo, M.D. Halls, J. Zhang, R.A. Friesner, Jaguar: A high-performance quantum chemistry software program with strengths in life and materials sciences, *Int. J. Quantum Chem.* 113 (2013) 2110–2142, doi:10.1002/qua.24481.
- [25] G.M. Morris, D.S. Goodsell, R.S. Halliday, R. Huey, W.E. Hart, R.K. Belew, A.J. Olson, Automated docking using a Lamarckian genetic algorithm and an empirical binding free energy function, *J. Comput. Chem.* 19 (1998) 1639–1662, doi:10.1002/(SICI)1096-987X(19981115)19:14<1639::AID-JCC10>3.0.CO;2-B.
- [26] N.M. Fahmy, E. Al-Sayed, S. Moghannem, F. Azam, M. El-Shazly, A.N. Singab, Breaking down the barriers to a natural antiviral agent: antiviral activity and molecular docking of erythrina speciosa extract, fractions, and the major compound, *Chem. Biodivers.* 17 (2020) e1900511–e1900511.
- [27] M.P. Jacobson, D.L. Pincus, C.S. Rapp, T.J.F. Day, B. Honig, D.E. Shaw, R.A. Friesner, A hierarchical approach to all-atom protein loop prediction, *Proteins* 55 (2004) 351–367, doi:10.1002/prot.10613.
- [28] M.P. Jacobson, R.A. Friesner, Z. Xiang, B. Honig, On the role of the crystal environment in determining protein side-chain conformations, *J. Mol. Biol.* 320 (2002) 597–608, doi:10.1016/S0022-2836(02)00470-9.
- [29] B. Vijayakumar, S. Parasuraman, R. Raveendran, D. Velmurugan, Identification of natural inhibitors against angiotensin I converting enzyme for cardiac safety using induced fit docking and MM-GBSA studies, *Pharmacogn. Mag.* 10 (2014) S639.
- [30] P.D. Lyne, M.L. Lamb, J.C. Saeh, Accurate prediction of the relative potencies of members of a series of kinase inhibitors using molecular docking and MM-GBSA scoring, *J. Med. Chem.* 49 (2006) 4805–4808.
- [31] Desmond Molecular Dynamics System, Schrödinger LLC, 2020.

- [32] K.J. Bowers, D.E. Chow, H. Xu, R.O. Dror, M.P. Eastwood, B.A. Gregersen, J.L. Klepeis, I. Kolossvary, M.A. Moraes, F.D. Sacerdoti, Scalable algorithms for molecular dynamics simulations on commodity clusters, in: *Proceeding of the SC '06: Proceedings of the 2006 ACM/IEEE conference on Supercomputing*, IEEE, 2006, p. 43.
- [33] E. Harder, W. Damm, J. Maple, C. Wu, M. Rebol, J.Y. Xiang, L. Wang, D. Lupyán, M.K. Dahlgren, J.L. Knight, OPLS3: a force field providing broad coverage of drug-like small molecules and proteins, *J. Chem. Theory Comput.* 12 (2016) 281–296.
- [34] W.G. Hoover, Canonical dynamics: method for simulations in the canonical ensemble, *Phys. Rev. A* 31 (1985) 1695–1697.
- [35] G.J. Martyna, D.J. Tobias, M.L. Klein, Constant pressure molecular dynamics algorithms, *J. Chem. Phys.* 101 (1994) 4177–4189.
- [36] D.D. Humphreys, R.A. Friesner, B.J. Berne, A multiple-time-step molecular dynamics algorithm for macromolecules, *J. Phys. Chem.* 98 (1994) 6885–6892.
- [37] B.A. Luty, M.E. Davis, I.G. Tironi, W.F. Van Gunsteren, A comparison of particle-particle, particle-mesh and ewald methods for calculating electrostatic interactions in periodic molecular systems, *Mol. Simul.* 14 (1994) 11–20, doi:10.1080/08927029408022004.
- [38] K.A. Dill, Additivity principles in biochemistry, *J. Biol. Chem.* 272 (1997) 701–704 <http://www.jbc.org/content/272/2/701.short>.
- [39] M. Ahmed, F. Azam, A. Gbaj, A.E. Zetrini, A.S. Abodlal, A. Rghigh, E. Elmahdi, A. Hamza, M. Salama, S.M. Bensaber, Ester prodrugs of ketoprofen: synthesis, in vitro stability, in vivo biological evaluation and in silico comparative docking studies against COX-1 and COX-2, *Curr. Drug Discov. Technol.* 13 (2016).
- [40] M.S. Hussain, F. Azam, K.F.H.N. Ahamed, V. Ravichandiran, I. Alkskas, Anti-endotoxin effects of terpenoids fraction from *hygrophila auriculata* in lipopolysaccharide-induced septic shock in rats, *Pharm. Biol.* 54 (2016), doi:10.3109/13880209.2015.1070877.
- [41] F. Azam, A.M. Amer, A. Rabulifa, M.M. Elzwawi, Ginger components as new leads for the design and development of novel multi-targeted anti-Alzheimer's drugs: a computational investigation, *Drug Des. Devel. Ther.* 8 (2014) 2045–2059, doi:10.2147/DDDT.S67778.
- [42] I.-L. Lu, N. Mahindroo, P.-H. Liang, Y.-H. Peng, C.-J. Kuo, K.-C. Tsai, H.-P. Hsieh, Y.-S. Chao, S.-Y. Wu, Structure-based drug design and structural biology study of novel nonpeptide inhibitors of severe acute respiratory syndrome coronavirus main protease, *J. Med. Chem.* 49 (2006) 5154–5161, doi:10.1021/jm060207o.
- [43] H. Yang, W. Xie, X. Xue, K. Yang, J. Ma, W. Liang, Q. Zhao, Z. Zhou, D. Pei, J. Ziebuhr, H. Hilgenfeld, K.Y. Yuen, L. Wong, G. Gao, S. Chen, Z. Chen, D. Ma, M. Bartlam, Z. Rao, Design of wide-spectrum inhibitors targeting coronavirus main proteases, *PLoS Biol.* 3 (2005) e324, doi:10.1371/journal.pbio.0030324.
- [44] F. Azam, I.M. Taban, E.E.M. Eid, M. Iqbal, O. Alam, S. Khan, D. Mahmood, M.J. Anwar, H. Khalilullah, M.U. Khan, An in-silico analysis of ivermectin interaction with potential SARS-CoV-2 targets and host nuclear importin α , *J. Biomol. Struct. Dyn.* (2020) 1–14, doi:10.1080/07391102.2020.1841028.
- [45] M. Sgobba, F. Caporuscio, A. Anighoro, C. Portioli, G. Rastelli, Application of a post-docking procedure based on MM-PBSA and MM-GBSA on single and multiple protein conformations, *Eur. J. Med. Chem.* 58 (2012) 431–440, doi:10.1016/j.ejmech.2012.10.024.
- [46] S. Genheden, U. Ryde, The MM/PBSA and MM/GBSA methods to estimate ligand-binding affinities, *Expert Opin. Drug Discov.* 10 (2015) 449–461, doi:10.1517/17460441.2015.1032936.
- [47] F. Azam, Elucidation of teicoplanin interactions with drug targets related to COVID-19, *Antibiotics* 10 (7) (2021) 856, doi:10.3390/antibiotics10070856.
- [48] A. Hospital, J.R. Goñi, M. Orozco, J.L. Gelpi, Molecular dynamics simulations: advances and applications, *Adv. Appl. Bioinform. Chem.* 8 (2015) 37–47, doi:10.2147/AABC.S70333.
- [49] E. Wang, H. Sun, J. Wang, Z. Wang, H. Liu, J.Z.H. Zhang, T. Hou, End-point binding free energy calculation with MM/PBSA and MM/GBSA: strategies and applications in drug design, *Chem. Rev.* 119 (2019) 9478–9508, doi:10.1021/acs.chemrev.9b00055.
- [50] A. Gahlawat, N. Kumar, R. Kumar, H. Sandhu, I.P. Singh, S. Singh, A. Sjöstedt, P. Garg, Structure-based virtual screening to discover potential lead molecules for the SARS-CoV-2 main protease, *J. Chem. Inf. Model.* 60 (2020) 5781–5793, doi:10.1021/acs.jcim.0c00546.
- [51] P. Avti, A. Chauhan, N. Shekhar, M. Prajapat, P. Sarma, H. Kaur, A. Bhat-tacharyya, S. Kumar, A. Prakash, S. Sharma, B. Medhi, Computational basis of SARS-CoV 2 main protease inhibition: an insight from molecular dynamics simulation based findings, *J. Biomol. Struct. Dyn.* (2021) 1–11, doi:10.1080/07391102.2021.1922310.
- [52] S. De Vita, M.G. Chini, G. Lauro, G. Bifulco, Accelerating the repurposing of FDA-approved drugs against coronavirus disease-19 (COVID-19), *RSC Adv.* 10 (2020) 40867–40875, doi:10.1039/D0RA09010G.
- [53] M.Z. Ahmed, Q. Zia, A. Haque, A.S. Alqahtani, O.M. Almarfadi, S. Banawas, M.S. Alqahtani, K.L. Ameta, S. Haque, Aminoglycosides as potential inhibitors of SARS-CoV-2 main protease: an in silico drug repurposing study on FDA-approved antiviral and anti-infection agents, *J. Infect. Public Health* 14 (2021) 611–619, doi:10.1016/j.jiph.2021.01.016.
- [54] S. Di Micco, S. Musella, M.C. Scala, M. Sala, P. Campiglia, G. Bifulco, A. Fasano, In silico analysis revealed potential anti-SARS-CoV-2 main protease activity by the zonulin inhibitor larazotide acetate, *Front. Chem.* 8 (2021) 1271 <https://www.frontiersin.org/article/>, doi:10.3389/fchem.2020.628609.
- [55] I. Maffucci, A. Contini, In silico drug repurposing for SARS-CoV-2 main protease and spike proteins, *J. Proteome Res.* 19 (2020) 4637–4648, doi:10.1021/acs.jproteome.0c00383.
- [56] A.A. Elmaaty, R. Alnajjar, M.I.A. Hamed, M. Khattab, M.M. Khalifa, A.A. Al-Karmalawy, Revisiting activity of some glucocorticoids as a potential inhibitor of SARS-CoV-2 main protease: theoretical study, *RSC Adv.* 11 (2021) 10027–10042, doi:10.1039/D0RA10674G.
- [57] S. Bhowmick, A. Saha, S.M. Osman, F.A. Alasmay, T.M. Almutairi, M.A. Islam, Structure-based identification of SARS-CoV-2 main protease inhibitors from anti-viral specific chemical libraries: an exhaustive computational screening approach, *Mol. Divers.* (2021), doi:10.1007/s11030-021-10214-6.
- [58] A. Parashar, A. Shukla, A. Sharma, T. Behl, D. Goswami, V. Mehta, Reckoning γ -glutamyl-S-allylcysteine as a potential main protease (mpro) inhibitor of novel SARS-CoV-2 virus identified using docking and molecular dynamics simulation, *Drug Dev. Ind. Pharm.* 47 (2021) 699–710, doi:10.1080/03639045.2021.1934857.
- [59] S. Bharadwaj, A. Dubey, U. Yadava, S.K. Mishra, S.G. Kang, V.D. Dwivedi, Exploration of natural compounds with anti-SARS-CoV-2 activity via inhibition of SARS-CoV-2 Mpro, *Brief. Bioinform.* 22 (2021) 1361–1377, doi:10.1093/bib/bbaa382.
- [60] M.A.A. Ibrahim, E.A.R. Mohamed, A.H.M. Abdelrahman, K.S. Allemail, M.F. Moustafa, A.M. Shawky, A. Mahzari, A.R. Hakami, K.A.A. Abdeljawaad, M.A.M. Atia, Rutin and flavone analogs as prospective SARS-CoV-2 main protease inhibitors: In silico drug discovery study, *J. Mol. Graph. Model.* 105 (2021) 107904, doi:10.1016/j.jmgm.2021.107904.
- [61] J. Prajapati, R. Patel, D. Goswami, M. Saraf, R.M. Rawal, Sterenin M as a potential inhibitor of SARS-CoV-2 main protease identified from MeFSAT database using molecular docking, molecular dynamics simulation and binding free energy calculation, *Comput. Biol. Med.* 135 (2021) 104568, doi:10.1016/j.combiomed.2021.104568.